Simple and sophisticated models of Taylor's cylinder impact

Sjue, Sky K.
Hickmann, Kyle Scott
Nguyen-Fotiadis, Nga Thi Thuy

To be published in:

DOI to publisher's version: 10.1063/12.0020511

Simple and Sophisticated Models of Taylor's Cylinder Impact

Sky Sjue,[a] Kyle Hickmann, and Nga Nguyen

Los Alamos National Laboratory, Los Alamos, New Mexico 87545, USA

[a] *Electronic mail: sjue@lanl.gov*

Abstract. We present a study based on the simplest possible models for Taylor's cylinder impact problem, in addition to examination of using convolutional neural networks (CNNs) to map cylinder profiles to strength calibrations. We find that the approximate treatments of Taylor and Hawkyard compare well with hydrodynamic simulations using an equivalent assumption of constant flow stress. The CNN models prove to be well suited to successfully infer parameterizations of the Preston-Tonks-Wallace model of plastic deformation based on the deformed profile of an impacted cylinder.

INTRODUCTION TO TAYLOR'S CYLINDER IMPACT

G. I. Taylor introduced the cylinder impact test [1] to estimate dynamic yield stresses in 1948. This yield-stress test fires a right cylinder of a material at a rigid anvil, with ideal conditions of constant initial velocity and a frictionless contact between the tested cylinder and the rigid anvil. Taylor provided arguments supporting approximations to estimate a constant yield stress from the final deformed length and undeformed length of a right cylinder after impact against a rigid anvil at a specified velocity. He based his approximations on considerations of the cylinder's momentum. J. B. Hawkyard proposed an alternate approximation based on considerations of the cylinder's kinetic energy [2] in 1968.

MOMENTUM FORMULATION

Consider a right cylinder of length L_0 fired at a rigid, unyielding anvil with initial velocity U, density ρ, radius R_0 and cross section A_0. Taylor outlined assumptions that the deformation happens instantaneously at the location of the plastic wave, where all material between the plastic wave and the impact surface has come to rest, and the remainder of the cylinder has time-dependent uniform velocity u.

We will only consider engineering strain, which can be written in terms of the area on either side of the plastic wave ($\varepsilon = 1 - A_0/A$), or velocity of the plastic wave v versus the rigid, undeformed cylinder's remaining velocity: $\varepsilon = u/(u+v)$. The velocity of the plastic wave can similarly be written in terms of the instantaneous cylinder velocity and deformation: $v = u(1-\varepsilon)/\varepsilon$. Newton's second law applied at the location of the plastic wave gives

$$\sigma(A - A_0) = \rho A_0 (u+v)u, \tag{1}$$

where σ is the flow stress, $\rho A_0(u+v)$ is the mass crossing the deformation boundary per unit time, and u is the velocity being brought to a halt. If we eliminate A, A_0, u and v in favor of ε, we find

$$\rho u^2/\sigma = \varepsilon^2/(1-\varepsilon), \tag{2}$$

which is instantaneously true at all times during the impact. The maximum strain ε_i is given by solving for ε with the initial condition $u = U$. The length of the undeformed portion of the cylinder is x, and we have $dx/dt = -(u+v)$. Newton's second law again applied to the undeformed portion of the cylinder gives $\sigma = -(\rho x)du/dt$. We can use the ratio of these two derivatives to write

$$\frac{dx}{du} = \frac{(u+v)\rho x}{\sigma} = \frac{\rho u x}{\sigma\varepsilon}; \qquad \frac{dx}{x} = \frac{\rho u du}{\sigma\varepsilon} = \frac{1}{2\varepsilon} d\left(\frac{\varepsilon^2}{1-\varepsilon}\right). \tag{3}$$

Integration by parts gives

$$2\ln(x) = \frac{\varepsilon}{1-\varepsilon} - \ln(1-\varepsilon) + c_0 = \frac{1}{1-\varepsilon} - \ln(1-\varepsilon) + c, \tag{4}$$

which uses the integration constants c_0 and $c = c_0 - 1$. Taking the definite integral over dx from L_0 to some smaller undeformed value x, one finds

$$\ln(x/L_0)^2 = \frac{1}{1-\varepsilon} - \frac{1}{1-\varepsilon_i} + \ln\left(\frac{1-\varepsilon_i}{1-\varepsilon}\right); \qquad \ln(X/L_0)^2 = 1 - \frac{1}{1-\varepsilon_i} + \ln(1-\varepsilon_i). \tag{5}$$

Together, Eqs. (2) and (4) determine the final undeformed length X as a function of the initial velocity U and the flow stress σ if we set $\varepsilon = 0$.

The height h of the plastically deformed portion of the cylinder grows as the plastic wave moves at velocity v, which we can combine with the rate of change of the undeformed length of the cylinder to obtain

$$\frac{dh}{dx} = \frac{-v}{u+v} = -1 + \varepsilon. \tag{6}$$

This equation is conceptually simple to integrate to find the cylinder's deformed profile

$$h = -\int_{L_0}^{x} (1-\varepsilon)dx; \qquad r(h) = R_0/\sqrt{1-\varepsilon}, \tag{7}$$

subject to solving for ε via Eq. (5) for each step dx. If this numerical integral is solved accurately, then the value of x when $\varepsilon = 0$ should agree with Eq. (4). Figure 1 illustrates this model in more detail, similar to Figure 1 in Taylor's 1948 article.

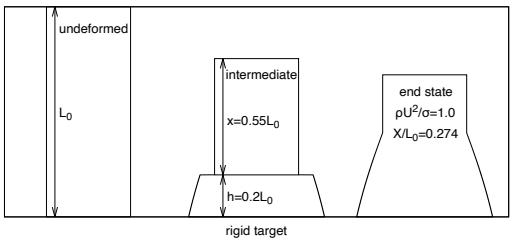

FIGURE 1. Taylor's model of a hypothetical copper cylinder impact with parameters $L_0 = 5$ cm, $L_0/R = 5$, σ=57.3 MPa, $\rho = 8.96$ g/cc and $U = 80$ m/s. The average strain rate from Eq. (10) in this case is $\dot{\varepsilon} \approx 1370\text{s}^{-1}$.

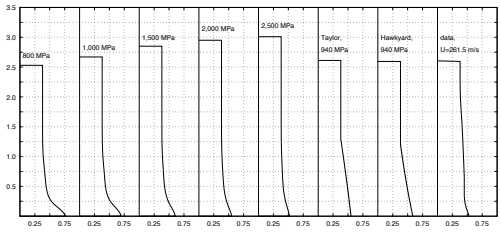

FIGURE 2. Constant flow stress simulations using FLAG Lagrangian hydrocode, compared to Taylor's simple model, Hawkyward's simple model, and actual data

FURTHER SIMPLIFYING ASSUMPTIONS

Taylor further assumed a constant plastic wave velocity and constant deceleration, to simplify solutions for expedited experimental estimates of flow stresses. If we assume a constant plastic wave velocity V, then we can manipulate Eq. (3) and integrate from $u = U$ to $u = 0$ to obtain

$$\frac{du}{dx} = \frac{\sigma}{\rho x(u+V)}; \qquad \frac{\sigma}{\rho}\ln(X/L_0) = -U^2/2 - VU. \tag{8}$$

If the final length of the cylinder is L_1, then we have $V = (L_1 - X)/T$. If the deceleration is constant, then the average velocity of the undeformed portion of the cylinder is $U/2 = (L_0 - L_1)/T$. These assumptions determine $V = (U/2)(L_1 - X)/(L_0 - L_1)$, which leads to Taylor's famous estimate of the yield stress

$$\sigma = \frac{\rho U^2}{2}\frac{1}{\ln(L_0/X)}\left(\frac{L_0 - X}{L_0 - L_1}\right). \tag{9}$$

This simple equation estimates the yield stress σ from the initial length L_0 and velocity U, based upon the final length L_1 and the undeformed length X. In practice, it can be difficult to determine X, because deformed profiles tend to be

smooth, especially as the strain approaches zero. Using these same assumptions, the average strain rate based on the average strain of the deformed portion divided by the duration of the plastic wave is

$$\dot{\varepsilon} = \frac{U}{2(L_0 - L_1)} \left(\frac{L_1 - X}{L_0 - X} \right). \tag{10}$$

ENERGY FORMULATION

Starting from the same assumption of instantaneous deformation bringing material to rest, Hawkyard notes that the plastic work per unit time is $\sigma(u+v)A_0 \ln(A/A_0)$, which creates internal energy in the stopped, deformed material. This comes from work per unit time arresting the rigid, undeformed portion of the cylinder, $\sigma u A_0$, and kinetic energy per unit time being lost into deformation, $A_0(u+v)\rho u^2/2$. Eq. (1) specified the rate of momentum loss due to the flow stress. Instead, we can equate the internal energy from plastic work in the deformed portion of the cylinder with the kinetic energy lost from the rigid, undeformed part:

$$\sigma(u+v)A_0 \ln\left(\frac{A}{A_0}\right) = \frac{\rho u^2}{2}(u+v)A_0 + \sigma A_0 u. \tag{11}$$

The analogy to Eq. (2) based on these work considerations is

$$(\rho/\sigma)u^2/2 = -\ln(1-\varepsilon) - \varepsilon, \tag{12}$$

which can again be solved for maximum strain ε_i based on the initial condition $u = U$. Unlike the quadratic Eq. (2), this one is transcendental. We take the differential of this equation and find

$$(\rho/\sigma)u\,du = d\varepsilon/(1-\varepsilon) - d\varepsilon = \varepsilon\, d\varepsilon/(1-\varepsilon). \tag{13}$$

None of the work considerations invalidate Eq. (3), so we use the differential of the work formulation with it to find

$$\frac{dx}{x} = \frac{\rho}{\sigma}\frac{u\,du}{\varepsilon} = \frac{d\varepsilon}{1-\varepsilon}; \qquad \ln(x) = -\ln(1-\varepsilon) + a; \qquad x = L_0(1-\varepsilon_i)/(1-\varepsilon), \tag{14}$$

where a is an integration constant based on $x = L_0$ when $\varepsilon = \varepsilon_i$, which is found before taking the exponential of both sides.

Now we write $v = dh/dt$ and use it with $\sigma = -(\rho x)du/dt$ to get

$$\frac{dh}{du} = -\frac{\rho x}{\sigma} v = -\frac{\rho x}{\sigma} u \frac{1-\varepsilon}{\varepsilon} = -\frac{\rho}{\sigma} u \frac{L_0(1-\varepsilon_i)}{\varepsilon}, \tag{15}$$

where first we used $v = u(1-\varepsilon)/\varepsilon$, then we used Eq. (14). Now we use the differential from Eq. (13) again

$$dh = -L_0(1-\varepsilon_i)d\varepsilon/(1-\varepsilon); \qquad h = L_0(1-\varepsilon_i)\ln(1-\varepsilon) + b; \qquad h = L_0(1-\varepsilon_i)\ln\left(\frac{1-\varepsilon}{1-\varepsilon_i}\right). \tag{16}$$

Here, b was another integration constant and this time it was found from the initial condition $h = 0$ when $\varepsilon = \varepsilon_i$. Taylor's momentum formulation required a numerical integral; Hawkyard's energy formulation results in a transcendental equation for the initial strain ε_i, then gives a closed form solution for the profile. This approach also allows a definite expression for the final length:

$$L_1 = L_0(1-\varepsilon_i) - L_0(1-\varepsilon_i)\ln(1-\varepsilon_i) = L_0(1-\varepsilon_i)[1 - \ln(1-\varepsilon_i)]. \tag{17}$$

CONSTANT FLOW STRESS SIMULATIONS

In order to test these simplest models in a case where some of the assumptions are valid, we simulated cylinder impacts for comparison using a constant flow stress model and a Lagrangian mesh in the FLAG hydrocode [3]. All of the simulations for comparison and CNN training are based on stainless steel 304L with a density $\rho = 7.91$ g/cc and

initial velocity $U = 261.5$ m/s, using the sesame equation of state 4272. Figure 2 shows simulated profiles for a range of flow stresses, profiles from Taylor and Hawkyard's theories, as well as actual data taken at LANL. Agreement on the final length L_1 was found from both theories using $\sigma = 940$ MPa. Using Eq. (10) and X from Taylor's theory with $\sigma = 940$ MPa, the average strain rate is estimated to be $\dot{\varepsilon} \approx 14,000\ \mathrm{s}^{-1}$.

Graphical summaries of the results on constant flow stress simulations are shown in Figs. 3 and 4. The final lengths L_1 from the models versus flow stress agree with simulated values significantly better than the maximum deformed radii. In Fig. 4, stress estimates from Eq. (9) applied to simulation results are shown compared with estimates based on the final calculated lengths. It is a nuisance to determine X for the estimate formula and we found it using the threshold $(R(X) - R_0)/(R_{\max} - R_0) = 0.05$, which was determined to give best agreement for this set of simulations. The consistency of the results suggests that either method is reasonable for conveniently estimating an average flow stress from a deformed cylinder length.

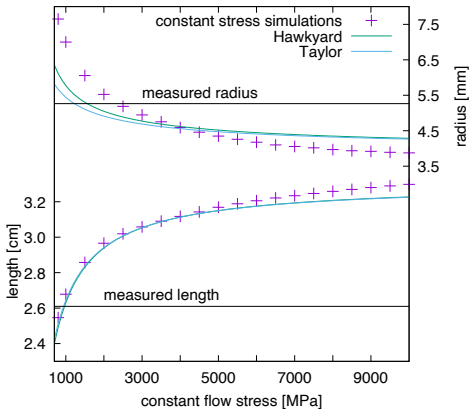

FIGURE 3. Comparison of constant flow stress simulation results to Taylor and Hawkyard's simple theories for final cylinder length (bottom left) and maximum deformed radius (top right).

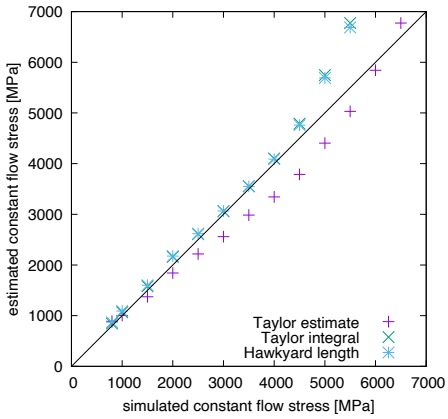

FIGURE 4. Taylor's more approximate estimate of the flow stress (Eq.(9)), results for flow stress based on numerical integration of Eq. (7) ("Taylor integral"), and stress from Hawkyard's deformed length (Eq. (17))

CONVOLUTIONAL REGRESSION ON THE PTW PARAMETERS

More realistic plastic behavior involves subtleties like strain hardening, strain-rate hardening, and thermal softening. The aspirational solution in this study is a regression model built with CNN layers used to learn how final cylinder profiles depend on Preston-Tonks-Wallace (PTW) strength model [4] parameters. First, we created our study data set that contains about 1,400 Taylor deformation profiles obtained from 1,400 corresponding samples of 8 parameters in the PTW model, γ, κ, p, s_0, s_∞, θ_0, y_0, and y_∞. From our set of simulated deformation profiles, we formed subsets for training, validation, and testing using 75% for training, 15% for validation, and 10% of the data for testing. Each profile was flattened into a series of 350 radial sampled along a regular grid in the z-coordinate (the cylinder axis). Thus, our training problem is to learn the mapping from the 350 radial profile values to the 8 PTW parameters.

We customized two one-dimensional convolutional regression architectures and evaluated the accuracy of the two models. Inspired by interpretable [5] learning, the first regression model (R_1) is built from repeated convolutional blocks that keep the filtered profile size approximately equal to the input profile size at each layer of the network. These *interpretable layers* are then followed by double-stride convolutional layers that quickly reduce the size of the profile, leading the network toward inferring the 8 PTW parameters. Once a predetermined, small, output length is reached dense regression layers are inserted to infer a final estimation of strength parameters. The number of filters N_k in the interpretable convolutional layers is kept small ($N_k = 12$). A total of 15 interpretable layers are used and then stride-2 layers are inserted until the output size is less than or equal to 20. This is followed by three dense layers having 10, 10, and 8 output neurons, respectively. In total this convolutional network uses only 12,000 parameters. However, R_1 extracts the nonlinear output/input relationship between the deformed profiles and simulation parameters with accuracy comparable to a much larger regression model (see Fig. 5 versus Fig. 6). Our second regression model,

R_2, is constructed with N_k being double in size after each computing unit consisting of 4 similar convolutional layers, starting with $N_k^i = 256$ and having $N_k^f = 1024$ in the final single convolutional block. A max-pooling layer is added after each convolutional multiplication aggressively reducing the resolution of inputs (from 350 in the first computing block to 21 in the final computing block). Consequently, R_2 has a much larger number of parameters ($\approx$ 5 million). High accuracy on the training set mirrored by comparable accuracy on the validation set is obtained after 5,000 epochs for R_1 and 20,000 epochs for R_2. Both models still exhibit limitations, with some data points in the test set exhibiting significantly lower accuracy compared to the majority of samples. Overall, R_2 performs slightly better than R_1 on all train, validation, and test sets but there are cases where R_1 outperforms R_2 as shown in Figure 7(a). Here, we compare the profile reconstruction using the predicted 8 PTW-parameters from two regression models R_1 (blue solid) and R_2 (purple solid) with ground truth (black solid). Other randomly selected samples of profile reconstruction (red solid) in the validation set obtained using predicted 8 PTW-parameters are shown in Figs. 7(b), (c), and (d).

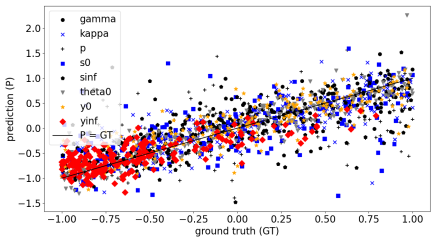

FIGURE 5. Prediction of 8 PTW-parameters (8 markers) on the validation set containing over 200 profiles using model with 12K hyper-parameters plotted in comparison to the ground truth values.

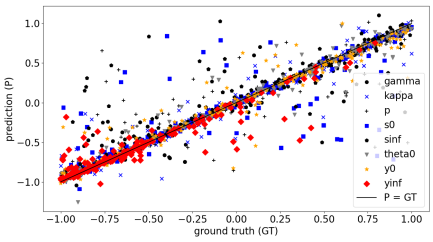

FIGURE 6. Prediction of 8 PTW-parameters (8 markers) on the validation set containing over 200 profiles using model with 5M hyper-parameters plotted in comparison to the ground truth values.

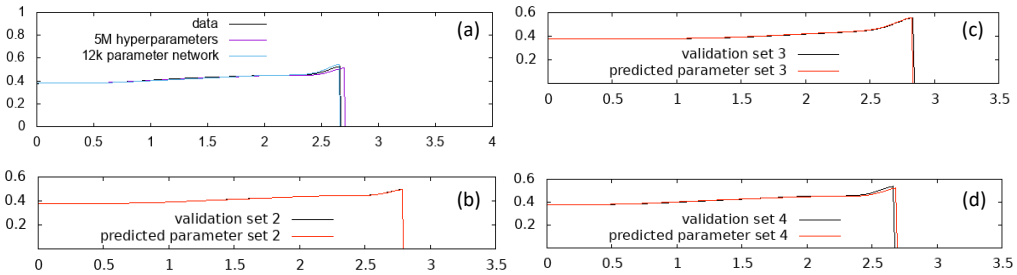

FIGURE 7. Post-impact profiles from simulations using predicted PTW parameters of both regression models (a) and from the wide regression model (b,c,d) compared to the ground truth profiles.

CONCLUSION

Both Taylor and Hawkyard's approximate treatment of the cylinder impact problem reproduce the maximum deformed radius and the final length of the cylinder well over a reasonable range of assumed constant flow stresses. The final total length is particularly well-suited to estimate the flow stress. Machine learning approaches with CNNs capture the relationship between parameterizations of the PTW model of plastic deformation and simulated cylinder profiles well. We propose application of this approach as a hybrid method when compared with traditional calibration and validation approaches. Often, a strength model like the PTW model is calibrated to quasi-static and split Hopkinson pressure bar stress-strain data, then validated by comparison with an impacted cylinder profile, which may reach higher strains and strain rates. Beginning with a Bayesian posterior set of models from traditional calibration data (*e.g.* [7]), it would be simple enough to train a network on these posterior parameter sets, then pick a final set based on the trained CNN applied to the profile data. This approach could also be generalized to more complex data sets that are still sensitive to strength, like Richtmyer-Meshkov or Rayleigh-Taylor instabilities driven by explosives.

ACKNOWLEDGMENTS

We are grateful for the support of the Advanced Radiography and Diagnostics Science Campaign at Los Alamos National Laboratory.

REFERENCES

1. G. I. Taylor, "The use of flat-ended projectiles for determining dynamic yield stress I. Theoretical considerations," Proceedings of the Royal Society A **194**: 289–299 (1948).
2. J. B. Hawkyard, "A theory for the mushrooming of flat-ended projectiles impinging on a flat rigid anvil, using energy considerations," International Journal of Mechanical Sciences **11**: 313–324 (1968).
3. D. E. Burton, "Lagrangian hydrodynamics in the FLAG code," Los Alamos National Laboratory, Los Alamos, NM, Technical Report No. LA-UR-07-7547 (2007).
4. Dean L. Preston, Davis L. Tonks and Duane C. Wallace, "Model of plastic deformation for extreme loading conditions," Journal of Applied Physics **93**, 211 (2003).
5. C. Molnar, Interpretable Machine Learning: A Guide for Making Black Box Models Explainable, 2nd ed. (self-published from Mucbook Clubhouse, Westendstraße 78, 80339 München, Germany 2022).
6. K. Simonyan and A. Zisserman, "Very deep convolutional networks for large-scale image recognition," arXiv:1409.1556 (2014).
7. Sky Sjue, James Ahrens, Ayan Biswas, Devin Francom, Earl Lawrence, Darby Luscher and David Walters, "Fast Strength Model Characterization Using Bayesian Statistics," AIP Conference Proceedings **2272**, 070043 (2020).